Title
Carbon sequestration potential on a reconnected floodplain: insights from the CosumnesRiver, California

Author
Clifton, Britne

Publication Date
2020-12-01

Title: Carbon sequestration potential on a reconnected floodplain: insights from the Cosumnes River, California

Investigator: Britne Clifton

Course: LA 227 – Restoration of Rivers and Streams

Document: Final Term Project – Second Draft

Date: December 18, 2020

1. Abstract:

Over a century of infrastructure implementation has instilled a sense of security against flooding that it comes as a surprise each time a levee is breached. Though the idea of controlling a river's force and flow took hold of generations before, recent developments in science and policy have included reconnecting floodplains to mitigate hazards. While flood mitigation is a valuable ecosystem service, studies of reconnected floodplains have expanded ecosystem service benefits to including biodiversity promotion, nutrient retention, and carbon sequestration in soils. However, few studies have considered the trapping and deposition of large woody debris (LWD) within floodplains or the potential role of LWD in various floodplain specific ecosystem services.

In this re-assessment of geomorphic change following a levee excavation that reconnected the Cosumnes River in Northern California, USA to its floodplain. The objective of the study was to evaluate the change across the floodplain since the excavation of the levee and determine the amount of LWD deposited in the area since. The assessment included mapping and measuring deposition of LWD as a baseline for future applications, tested the application of reflectance classification in LWD identification, and calculated the carbon stock

available within a deposit. At this restoration site, a single LWD deposit can trap 326.5 Mg of C (carbon). This work intends to inform research for the Cosumnes River Experimental Floodplain and potentially provide methods applicable to floodplains elsewhere.

2. Introduction:

In the last century and half, society has invested billions of dollars in infrastructure to control river systems around the world. Infrastructure including dams, dikes, and levees were built to separate rivers from property and protect society from flooding. In California's Central Valley (the Valley herein), the dynamic geological history has created some of the richest floodplains in the world. Through millennia of seismic activity, the Valley created by surrounding mountain ranges is almost completely disconnected from its outlet to the sea. The Valley's fertility lands and abundant water have drawn millions of people, leading to urban populous centers and rural agriculture worth billions to the state economy (CDFA, 2020). California now has over 7000 km levees, just over 5000 of those are within the Sacramento-San Joaquin Delta and watersheds (USACE, 2018; Water Resources, 2020; CVFPP, 2017). The extensive infrastructure fails to prevent the Central Valley from frequently being the site of devastating floods, that consistently result in billions of dollars of damage and, sometimes, loss of life (Mount, 2017). With the cycle of investment in infrastructure increasing control on water and ultimate failure of infrastructure, which drives subsequent cycling, novel approaches have become the focus of investigation by scientists and application by practitioners such as reconnecting floodplains for flood mitigation.

While studies have investigated flood mitigation through floodplain reconnection by setting-back and/or excavating levees (Serra-Llobet, Kondolf, Schaefer, & Nicholson, 2018; Swenson, Whitener, & Eaton, 2003), others have expanded to included floodplain restoration (Nichols & Viers, 2017; Scheel, 2018), recovery of ecological processes (Ciotti, McKee, Pope, Kondolf, & Pollock, 2020), river geomorphology re-establishment (Florsheim & Mount, 2002;

Nienhuis, Törnqvist, & Esposito, 2018; Whipple & Viers, 2019), sediment recharge (Pringle, 2003), and riparian corridor refugia re-establishment (Andrews, 1999; Stephens & Rockwell, 2019). However, the value of reconnected floodplains discussed thus far in literature fails to investigate carbon stock availability in large woody debris (LWD) and its potential influence on various floodplain processes.

To investigate this gap in knowledge, this study evaluated a process-based restoration project initiated in 2014 that excavated a levee and reconnected an experimental floodplain (floodplain herein) to the lower Cosumnes River (Nichols & Viers, 2017). The objective of this evaluation is to investigate the geomorphic change that has occurred across the floodplain and investigate the development of contributing factors or services since the excavation, such as volume and carbon stock of LWD.

3. Methods

3.a. Study Site:

The Cosumnes River is considered an unimpaired river (only levees and surrounding agricultural irrigation withdrawal lowering the water table) that runs from the lower Sierra Nevada (90 % rain fed) to its confluence with the Mokelumne River just before the Sacramento-San Joaquin Delta. While flood pulses can be as great as 36,000 cubic feet per second, the rain fed nature of the Cosumnes River typically results in a dry channel by August. The reconnected experimental floodplain lies within the Cosumnes River Preserve, owned by The Nature Conservancy, and as such, has decades of restoration initiatives with various success rates, including other reconnected floodplains (Florsheim & Mount, 2002; Nichols & Viers, 2017; Swenson et al., 2003). Focusing on the 2014 project's excavation site adjacent to the channel, we applied the following methods to determine the extent of woody debris deposition present and measure carbon stock available.

3.b. Study Focus - Restoration Project:

In 2011, the final Biological Technical Report, which laid out the excavation and reconnection to the Cosumnes River to be deployed in 2014, restoration objectives, and key beneficial effects of the proposed project was submitted for the Oneto-Denier Floodplain and Habitat Restoration Project (AECOM, 2011). The restoration of roughly 600 acres of riparian forest habitat, restoration of natural floodplain processes, increased aquatic/riparian habitat during inundation, increased food and resources for species (food-web productivity), increased species diversity, and the maintenance/improvement of ecological integrity (because of flood pulse impact) were the primary goals cited (AECOM,2011). Nichols & Viers (2016) created the pre-restoration baseline just prior to the 2014 excavation and compared it to the 2015 post-excavation physical characteristics and geomorphic change across the floodplain within the first year, which contextualized the various objectives originally proposed by the restoration project. Focusing on the 2014 project's excavation site adjacent to the channel and the subsequent geomorphic change, we applied the following methods to determine the extent of woody debris deposition present and measure carbon stock available.

For this study, we revisited the site of the 2014 excavation and the floodplain. Surveys for LWD, including measuring and cataloging data.

3.c Data Collection and Geomorphic Change Detection:

LiDAR data was collected on 10 September 2020 using a DJI M600 UAV with a Phoenix AL3-32 LiDAR sensor. Data was processed, verifying by comparing to reference sites available for both years, and limited to the extent of the 2014 excavation which resulted in a .las file including points from all returns for the study area. The 2020 LiDAR data and 2014 RTK derived point clouds were used to create a DEM (digital elevation model), DTM (digital terrain model), and DSM (digital surface model).

We calculated the difference between 2020 surface elevation and 2014 surface elevation using the DTM from post-excavation 2014 and the DTM for 2020 resulting in a DEM of Difference (DoD; in meters) (Wheaton, Brasington, Darby, & Sear, 2010). This DoD was used to evaluate the geomorphological change over the study period. **Figure 1** depicts the resulting difference in elevation in meters, interpreted as geomorphic change caused by river processes since the 2014 excavation, range from more than 1 meter of excision depicted in blue to deposition up to 1.6 meters depicted in pink.

DoD from the difference between the 2020 DEM and the 2020 DTM was applied to create 2020 above ground material (AGM). The 2020 above ground biomass informed calculations for LWD after field deployment surveying.

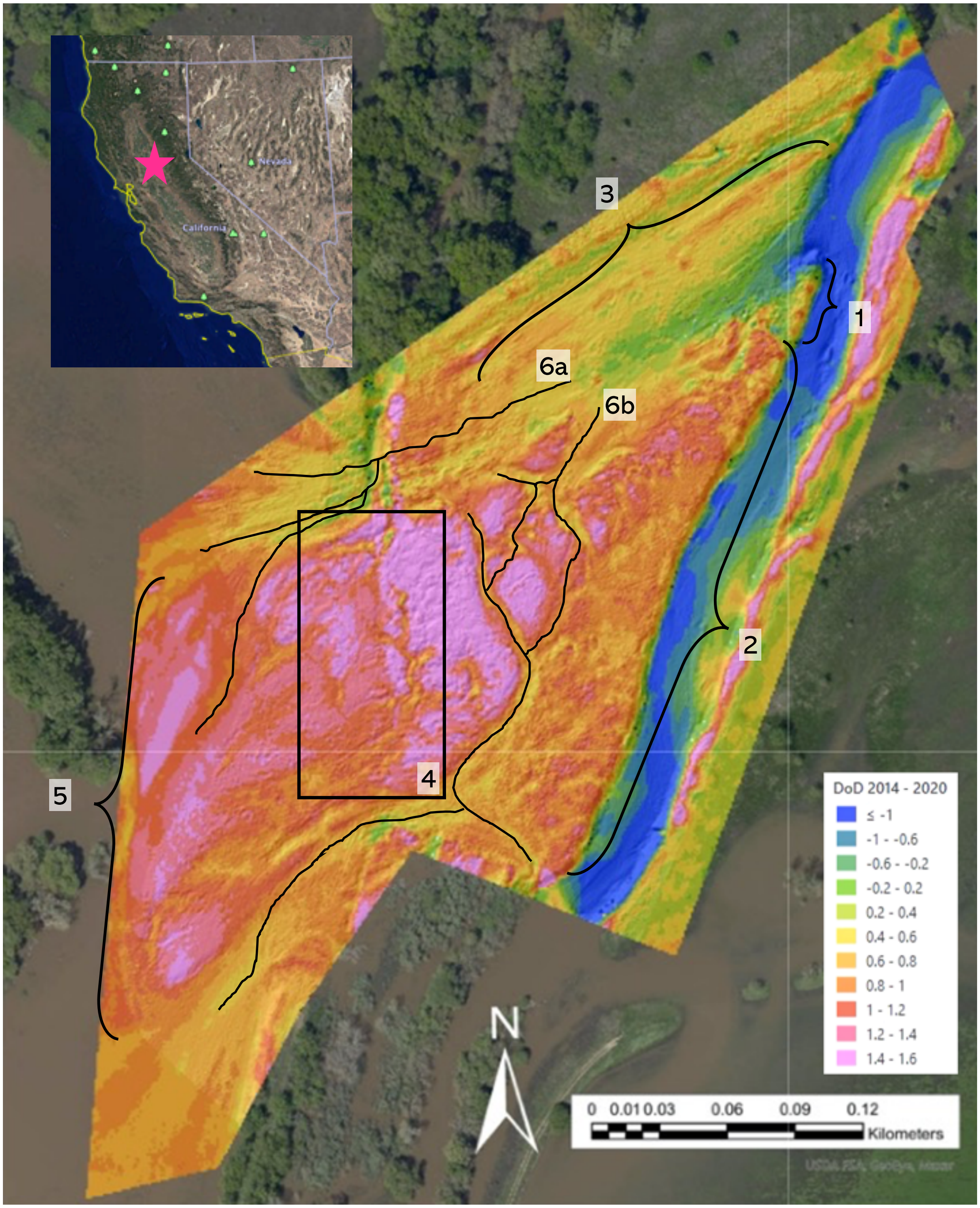

Figure 1 *DoD in meters between 2014 and 2020 of the excavation site and reconnected floodplain. The areas of deposition can be seen in warm tones up to 1.6 m and excision is depicted up to -1m in cool tones. Areas of deposition across the floodplain (up to pink) are depicted at the transect of the floodplain and channel (1) and at the boundary between the channel and the floodplain (2). The dynamics produced my excision at the confluence and deposition based on flow appears to have created a natural levee formation as seen in (3). Because a grove of willows (4) was left during the excavation in 2014, extensive deposition can be seen around (4) and the resulting subsequent sand splay (5) from levee removal above and below the grove, as well as the introductory evidence of potential secondary channel formation at (6a) and (6b). The characteristics of (1) and (2) also align with the areas of LWD, with the focus of this study limited to the deposition of LWD within (1).*

3.d. Data Collection:

Focusing on areas of deposition in Figure 1 and visually exploring open access imagery provided by the google earth application we identified LWD data collection points, displayed in **Figure 2**. We prioritized locations by size of deposit, with coordinates saved to a Google Maps file for field deployment. Target information in data collection included: (1.) Location ID and perimeter/point of large deposits using TopNet RTK gps positioning hardware including a handheld Rover sensor and TopCon devise, (2.) Extensive photographic data with ID information, (3.) Per point: length and circumference at both ends for the largest and smallest tree or branch available or length and circumference 4 ft above root line if both ends are not accessible (for largest tree/branch) (4.) Any species ID possible for any piece in the deposit (i.e., soft/woody >> pine, oak >> valley oak, cottonwood >> specific species of willow). Data collection included the following equipment: ground-based rtkGPS survey sensor and TopCon, standard soft tape measure, field guide with region specific plant species information, Google

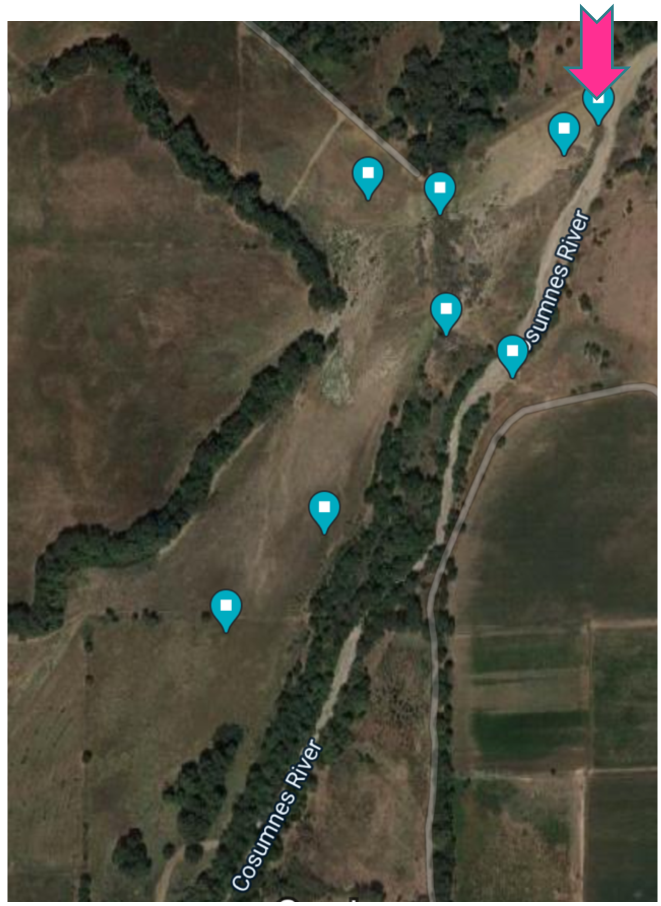

Figure 2 *The locations designated for LWD survey during field work. Each location displayed deposition from visual analysis of aerial photogrammetry. Areas of survey focused near the excavation site and area of reconnection to the channel due to large amounts of LWD deposition visible, limited time/resource availability, the potential to verify the conceptual framework of Nichols and Viers (2016) and remain within their study area of the 2014/2015 evaluation.*

Maps v10.56.1 application with saved deposit location file, and Camera application on an Apple iPhone 11 Pro. For the extent of this study, the location emphasized in figure 2 by the large pink arrow, the deposit at the confluence of the channel and floodplain (Figure 1 location 1), was the focus location. Photographic examples of data collection can be found in **Appendix C**.

3.e. LWD Identification:

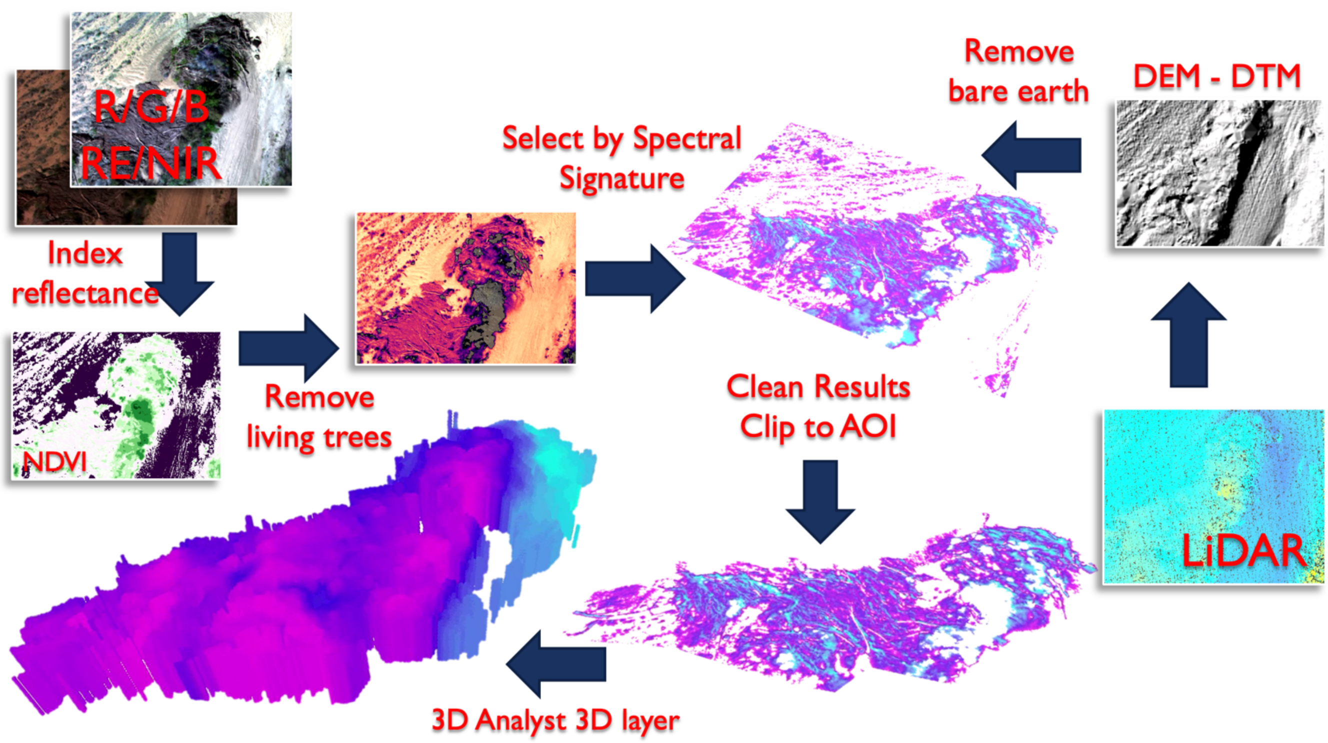

Figure 3 NDVI band calculation results indicated that LWD reflected in both RED and NIR band widths differently than the living material and the sediment surrounding the LWD. Using this spectral signature, we removed NDVI values greater than .4 using the 'clip' ArcGIS base tool. The 2014-20 DoD, 2020 AGM, and 2020 band files were each masked by the NDVI value parameter, as discussed above, and any outlying pixels were manually selected through shape extraction. This clipped extent 2020 DSM and 2020 DTM are then used for the 'Polygon Volume' function in ArcGIS Pro's 3D Spatial Analyst license which provides the Area and Volume toolset (ESRI, 2020) to determine the volume of material above ground level shown in Figure 4. The workflow applied here is based on the methods provided by Stal et al., 2010.

2020 Multispectral data was collected using a Mica Sense Red Edge 5 band sensor attached to a fixed-wing UAV on 22 September 2020. The collected data was processed, corrected, and validated for the study site using Pix4D v4.6.3 processing software which resulted in 5 individual band (blue, green, red, red edge, NIR) TIFF files. We visually assessed individual reflectance bands and various band combinations for anomalies and to determine if LWD had spectral signature by identifying reflectance values at any wavelength or combination. Normalized Difference Vegetation Index (NDVI) was calculated using red and NIR bands using the ENVI v5.5 (HGS, 2020) NDVI calculator tool, validated by applying band calculations tool for the NDVI equation using RED and NIR bands (Harris, 2018). While we applied bare-earth corrected NDVI and other band combination calculations, the difference between LWD and living plant material in standard NDVI proved the most valuable for differentiating LWD from surrounding material (Mukaromah, As-syakur, & Prastowo, 2019).

3.f. Calculate Carbon Content

Because reflectance values between LWD and living plants varied greatly in the NIR exclusion of leafy plant material was possible, specifically with the exclusion of NDVI values over 0.4, the point and parameter data collected in the field validates reflectance findings and prevents over-exclusion in the deposit. The resulting volume, 2105.73 m^3, is then corrected to 50% to account for void space between logs resulting in 1052.87 m^3. That result, which is considered the total volume of wood material available in the deposit, is multiplied by the density of *Populus fremontii* and *Quercus lobata* (Fremont Cottonwood and Valley Oak most common for this reach), 627.5 kg/m^3, resulting in a mass of 660.66 Mg. We use the 660.99 Mg calculate carbon content within the LWD by multiplying by 49.41%, which is the average carbon content of the common species (Asner & Mascaro, 2014; Campbell et al., 2019; Coomes et al., 2017).

4. Results:

The reconnection of the floodplain allowed geomorphological changes across the excavated site as seen in the 2014-2020 DoD (Figure 1). Figure 1 depicts the resulting change including the extent and location of excision, deposition, and the development of crevasse and sand splay. Comparing the 2014-2020DoD and 2020 above ground material (AGM) at the intersection of the floodplain and channel indicated high deposition that mirrored the survey focus.

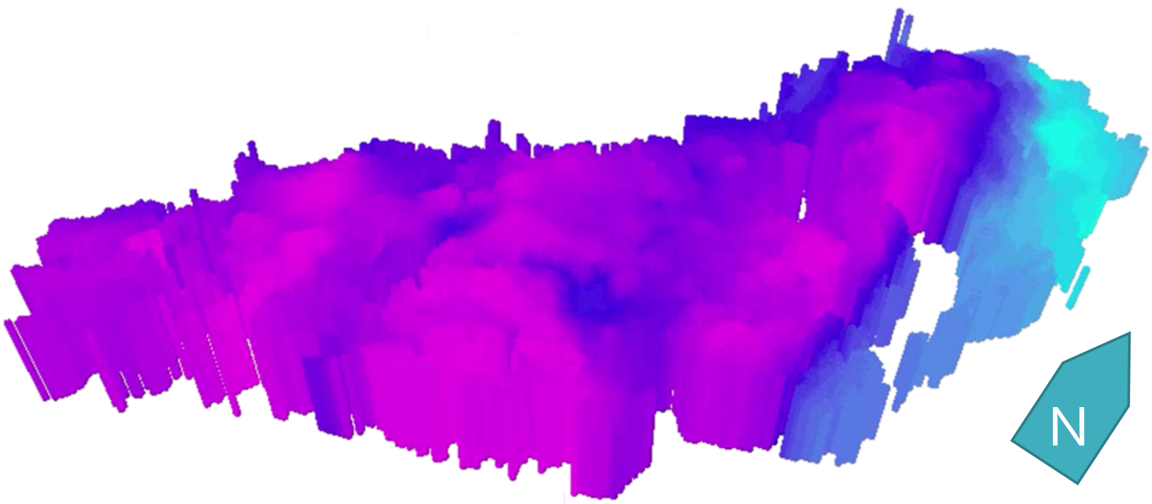

Figure 4 *A 3D rendered version of the LWD deposit at the confluence of the channel and reconnected floodplain. Referenced location and color are reflected in Appendix D.*

Once the calculations were completely, we determined that the resulting carbon content of the deposit in **Figure 4** is 326.5 Mg.

Figure 5 provides context to the size of the deposit at the junction between the floodplain and channel, also the largest deposit by height, measured in Figure 4.

Figure 5 *Large woody debris deposit at the confluence of the channel and the reconnected floodplain. The researcher in the image is ~1.7 meters tall for reference. This deposit is the focus of this study, though not the only deposit on this reconnected floodplain.*

5. *Discussion:*

This re-assessment of change detection following the excavation at the Cosumnes River Experimental Floodplain in 2014 included measuring the geomorphic change across the floodplain. Following the workflow of Nichols and Viers (2016) and applying the theoretical framework provided by Florsheim and Mount (2002) - Appendix A - and Nichols and Veirs (2016) – Appendix B, geomorphic change detection through the DoD depicts results align with the frameworks as expected. Figure 1 includes a distinct incision expanding onto the floodplain at the northern end of the excavated region adjacent to the channel that decreases in depth as it extends onto the floodplain. Though the erosion depth decreases, there is a depression that continues onto the floodplain that expands into multiple smaller depressions in the sediment seeming to be the beginning of a braided network and the foundation of a secondary channel.

While the LWD at the channel confluence aligns with expectations of Nichols and Viers's (2016) theoretical framework, there is far less discussion found within the literature of LWD deposition across the floodplain, its impact on the floodplain itself, and as an ecosystem service. Instead, LWD is considered a temporary variable that belongs to river studies because they will inevitably rejoin the channel, thus only mentioned in passing (Wohl, 2020). Additionally, carbon budget influences are discussed in other areas of reconnected floodplain dynamics including soil composition on the Cosumnes River Experimental Floodplain (Dybala, Matzek, Gardali, & Seavy, 2019; Dybala, Steger, et al., 2019; Matzek, Stella, & Ropion, 2018; Stella et al., 2011), but LWD is lacking from the literature discussion. At 326.5 Mg for a single deposit, further investigation is necessary to determine comparative value to other factors within the carbon budget. While determining the volume of LWD within a deposit is informative, the extent of deposition and the conditions created by the LDW extends beyond the confluence as outlined in Appendix A.

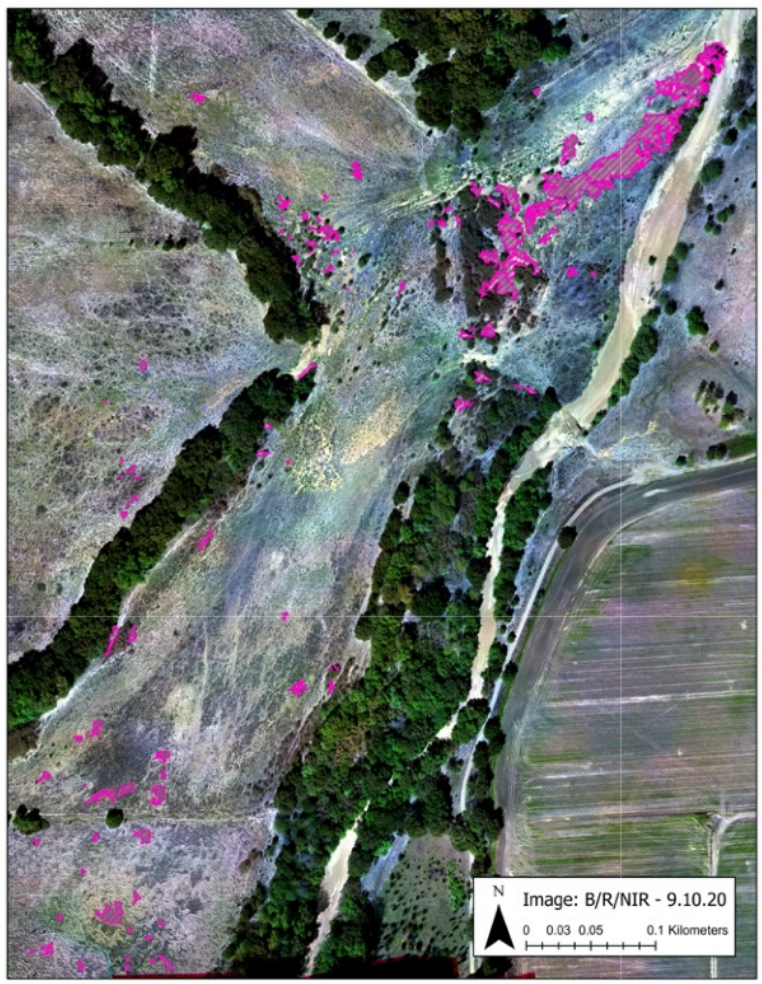

Figure 6 *Highlighted areas are LWD deposits across the floodplain.*

The extent of LWD visible across the floodplain in **Figure 6** contextualizes the spread of LWD into areas where LWD residence time could be much longer than a single dry season. If this debris is entrapped on the floodplain, the residence time could ultimately result in the LWD providing services such as those LWD provides to channel form and dynamics (Wohl, 2019), or being buried by sediment deposition or being a sediment trap. While the literature lacks LWD floodplain residence time discussions, the potential of LWD to be able to provide services across a floodplain influencing floodwater residence time, sediment deposition, carbon sequestration (either direct or support of), local primary production, and temporary habitat /refugia during flood events for invertebrates and small or juvenile fish provides justification to pursue this research further with.

6. Conclusions:

Floodplain reconnection and restoration holds promise for its potential ecological and social benefits, as well as flood risk management. As flood hazards are projected to increase in number and magnitude in coming decades due to climate change, floodplain reconnection is gaining support as approaches to manage flood risk with other multiple benefits. Additional ecosystem services further support and encourage investment in floodplain reconnection. Our research showed that the floodplain reconnected to the Cosumnes River in 2014 restored geomorphic processes of river flow dynamics' access to floodplains during high flow events and resulted in storage and sequestration of carbon on the floodplain due to retention of LWD. While preliminary analysis of the LWD deposit, a fraction of the LWD identified in satellite imagery and LiDAR surveys, on the restored site have identified a previously uncatalogued 326.9 Mg C. Further assessment of carbon stocks based on the methods established in this study will yield a poorly understood carbon sink provided by floodplain reconnection, both at the Cosumnes River floodplain and other floodplains in the region.

*References Cited (fix the **bolded** ones):*

AECOM. (2011). Denier II/Oneto Property Floodplain and Riparian Habitat Restoration Project. Final Biological Technical Report. Sacramento, CA: The Nature Conservancy.

Alden, H. A. (1995). Hardwoods of North America. FPL-GTR-83. *Madison, WI: USDA Forest Service, Forest Products Laboratory*.

Andrews, E. S. (1999). Identification of an ecologically based floodway: the case of the Cosumnes River, California. In S. B. Marriott & J. Alexander (Eds.), *Floodplains: Interdisciplinary Approaches* (pp. 99–110). London: Geological Society, London.

Asner, G. P., & Mascaro, J. (2014). Mapping tropical forest carbon: Calibrating plot estimates to a simple LiDAR metric. *Remote Sensing of Environment*, *140*, 614–624. https://doi.org/10.1016/j.rse.2013.09.023

Campbell, J. L., Green, M. B., Yanai, R. D., Woodall, C. W., Fraver, S., Harmon, M. E., … Domke, G. M. (2019). Estimating uncertainty in the volume and carbon storage of downed coarse woody debris. *Ecological Applications*, *29*(2), 1–13. https://doi.org/10.1002/eap.1844

Ciotti, D., McKee, J., Pope, K., Kondolf, G. M., & Pollock, M. (2020). Process-based design criteria for restoring fluvial systems. *BioScience*.

Coomes, D. A., Dalponte, M., Jucker, T., Asner, G. P., Banin, L. F., Burslem, D. F. R. P., … Qie, L. (2017). Area-based vs tree-centric approaches to mapping forest carbon in Southeast Asian forests from airborne laser scanning data. *Remote Sensing of Environment*, *194*, 77–88. https://doi.org/10.1016/j.rse.2017.03.017

Dybala, K. E., Matzek, V., Gardali, T., & Seavy, N. E. (2019). Carbon sequestration in riparian forests: A global synthesis and meta-analysis. *Global Change Biology*, *25*(1), 57–67.

https://doi.org/10.1111/gcb.14475

Dybala, K. E., Steger, K., Walsh, R. G., Smart, D. R., Gardali, T., & Seavy, N. E. (2019). Optimizing carbon storage and biodiversity co-benefits in reforested riparian zones. *Journal of Applied Ecology*, *56*(2), 343–353. https://doi.org/10.1111/1365-2664.13272

Florsheim, J. L., & Mount, J. F. (2002). Restoration of floodplain topography by sand-splay complex formation in response to intentional levee breaches, Lower Cosumnes River, California. *Geomorphology*, *44*(1–2), 67–94. https://doi.org/10.1016/S0169-555X(01)00146-5

Harris Geospatial Solutions, Inc. (2020) - L3HARRIS ENVI Software. Bloomingfield, CO

Lamlom, S. H., & Savidge, R. A. (2003). A reassessment of carbon content in wood: Variation within and between 41 North American species. *Biomass and Bioenergy*, *25*(4), 381–388. https://doi.org/10.1016/S0961-9534(03)00033-3

Matzek, V., Stella, J., & Ropion, P. (2018). Development of a carbon calculator tool for riparian forest restoration. *Applied Vegetation Science*, *21*(4), 584–594. https://doi.org/10.1111/avsc.12400

Mukaromah, L., As-syakur, A. R., & Prastowo, E. (2019). Opportunities for the application of Red-edge reflectance- based indices in coastal vegetation and agro-ecological studies, *5*, 251–259.

Nichols, A. L., & Viers, J. H. (2017). Not all breaks are equal: Variable hydrologic and geomorphic responses to intentional levee breaches along the lower Cosumnes River, California. *River Research and Applications*, *33*(7), 1143–1155. https://doi.org/10.1002/rra.3159

Nienhuis, J. H., Törnqvist, T. E., & Esposito, C. R. (2018). Crevasse Splays Versus Avulsions: A Recipe for Land Building With Levee Breaches. *Geophysical Research Letters*, *45*(9), 4058–4067. https://doi.org/10.1029/2018GL077933

Pringle, C. (2003). What is hydrologic connectivity and why is it ecologically important? *Hydrological Processes*, *17*(13), 2685–2689. https://doi.org/10.1002/hyp.5145

Scheel, K. (2018). *Toward Understanding Changes in Large-Sale Floodplain Connectivity Caused by Levee*. Colorado State University.

Serra-Llobet, A., Kondolf, G. M., Schaefer, K., & Nicholson, S. (2018). *Managing Flood Risk: Innovative Approaches from Big Floodplain Rivers and Urban Streams*. *Managing Flood Risk: Innovative Approaches from Big Floodplain Rivers and Urban Streams*. https://doi.org/10.1007/978-3-319-71673-2

Stella, J. C., Hayden, M. K., Battles, J. J., Piégay, H., Dufour, S., & Fremier, A. K. (2011). The Role of Abandoned Channels as Refugia for Sustaining Pioneer Riparian Forest Ecosystems. *Ecosystems*, *14*(5), 776–790. https://doi.org/10.1007/s10021-011-9446-6

Stephens, J. L., & Rockwell, S. M. (2019). Short-term riparian restoration success measured by territory density and reproductive success of three songbirds along the Trinity River, California. *Gerontologist*, *59*(4), 1–12. https://doi.org/10.1093/condor/duz043

Swenson, R. O., Whitener, K., & Eaton, M. (2003). Restoring floods on floodplains: riparian and floodplain restoration at the Cosumnes River Preserve. *California Riparian Systems: Processes and Floodplain Management, Ecology, Restoration, 2001 Riparian Habitat and Floodplains Conference Proceedings, Faber PM (Ed.). Riparian Habitat Joint Venture: Sacramento, CA*, (April), 224–229. Retrieved from http://www.sjrdotmdl.org/concept_model/phys-chem_model/documents/300001823.pdf

Wheaton, J. M., Brasington, J., Darby, S. E., & Sear, D. A. (2010). Accounting for uncertainty in DEMs from repeat topographic surveys: Improved sediment budgets. *Earth Surface Processes and Landforms*, *35*(2), 136–156. https://doi.org/10.1002/esp.1886

Whipple, A. A., & Viers, J. H. (2019). Coupling landscapes and river flows to restore highly modified rivers. *Water Resources Research*, *55*, 4512–4532. https://doi.org/10.1029/2018WR022783

Wohl, E. (2019) Rivers in the Landscape. Wiley-Blackwell; 2nd Edition. ISBN: 1119535417

Figures with Captions:

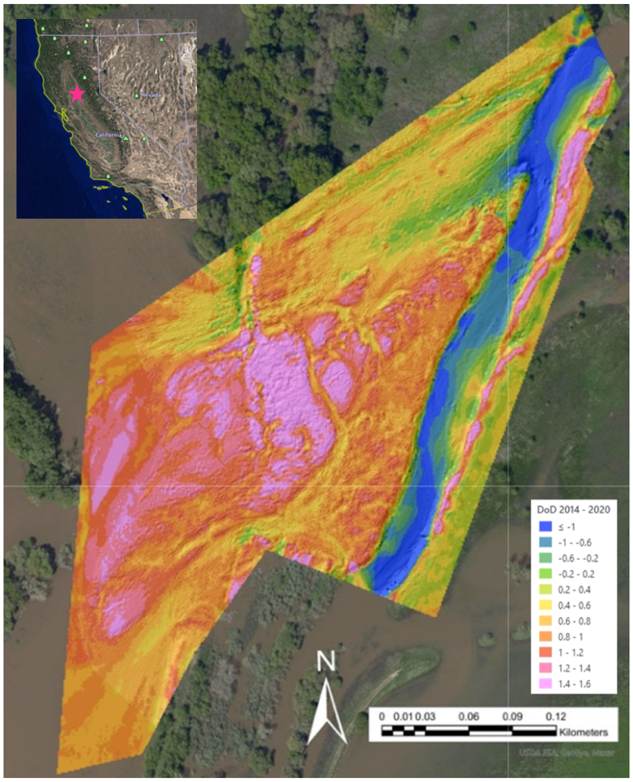

Figure 1 *DoD (DEM of Difference) between 2014 and 2020 the excavation site and reconnected floodplain. The areas of deposition can be seen in warm tones up to 1.6 m and excision is depicted up to -1m in cool tones. Several areas in the center appear to be possible secondary channel formations while a naturally forming levee is forming in the northern region of the floodplain as well. Indicators of channel meander are expressing within the channel just south of the reconnection.*

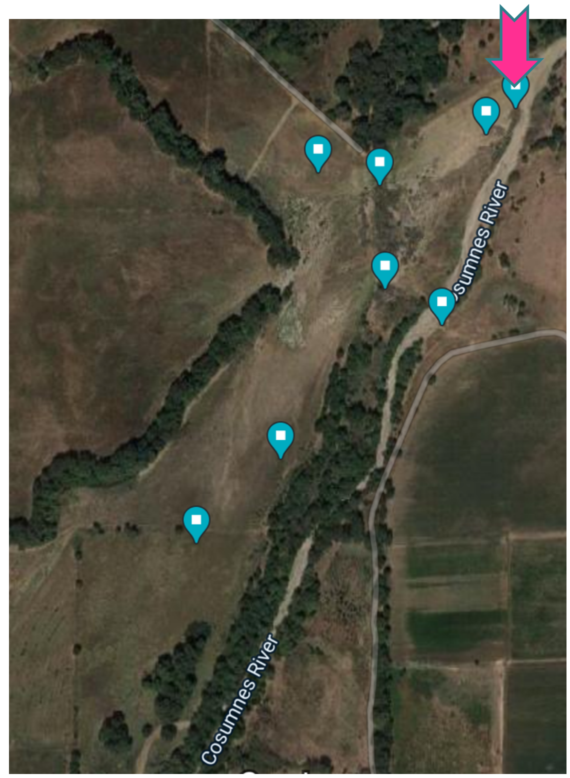

Figure 2 *The locations designated for LWD survey during field work. Each location displayed deposition from visual analysis of aerial photogrammetry. Areas of survey focused near the excavation site and area of reconnection to the channel because of increased amounts of*

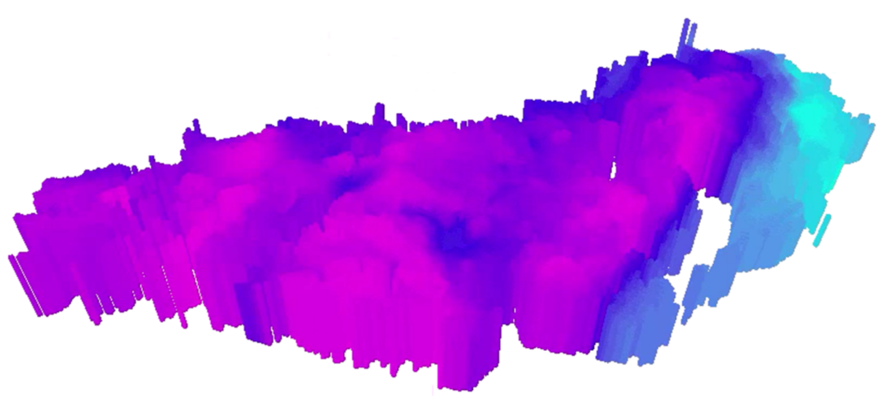

Figure 4 *A 3D rendered version of the LWD deposit at the confluence of the channel and reconnected floodplain.*

Figure 5 *Large woody debris deposit at the confluence of the channel and the floodplain. The researcher in the image is ~1.7 meters tall for reference. This deposit is the focus of this study, though not the only deposit on this floodplain*

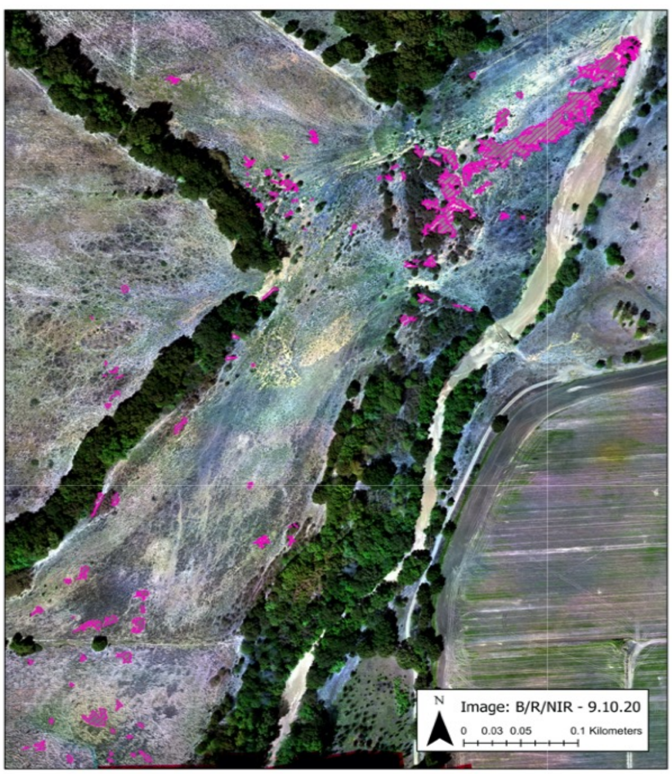

Figure 6 Highlighted areas of LWD deposition across the floodplain.

Appendices:

Appendix A:

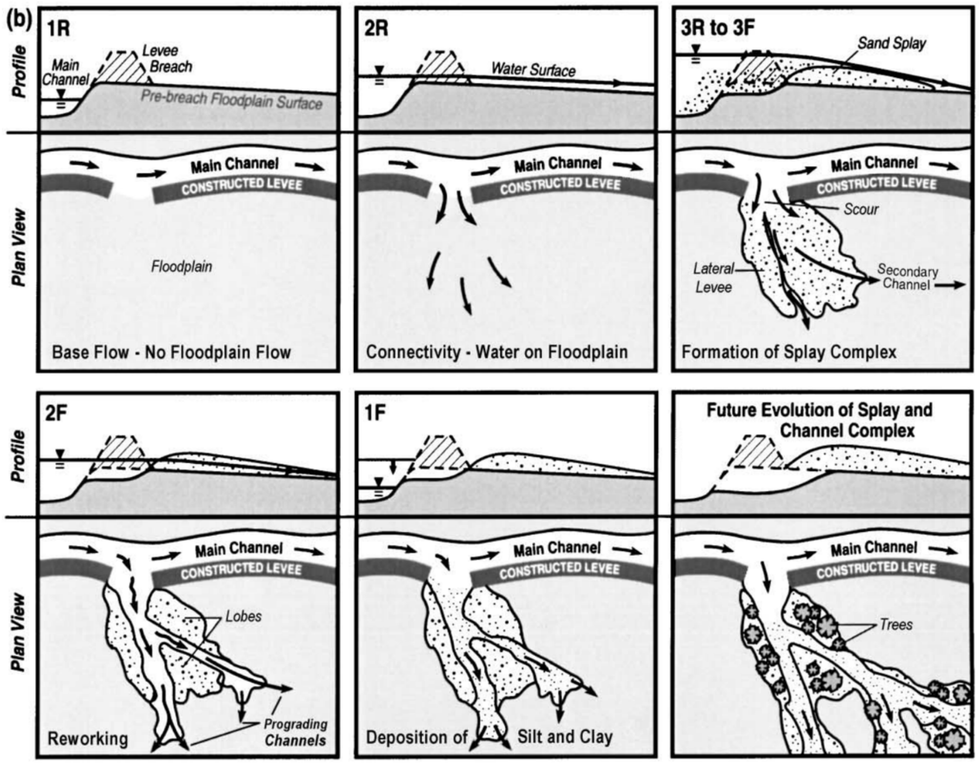

Fig. 15. Conceptual model describing sand-splay complex formation and development of floodplain topography. (a) Development of floodplain topography is related to three rising (1 to 3R) and falling (3 to 1F) stages of the hydrograph. (b) Schematic profiles and maps describing stages of evolution of floodplain topography are correlated with six stages of the conceptual hydrograph.

Appendix B:

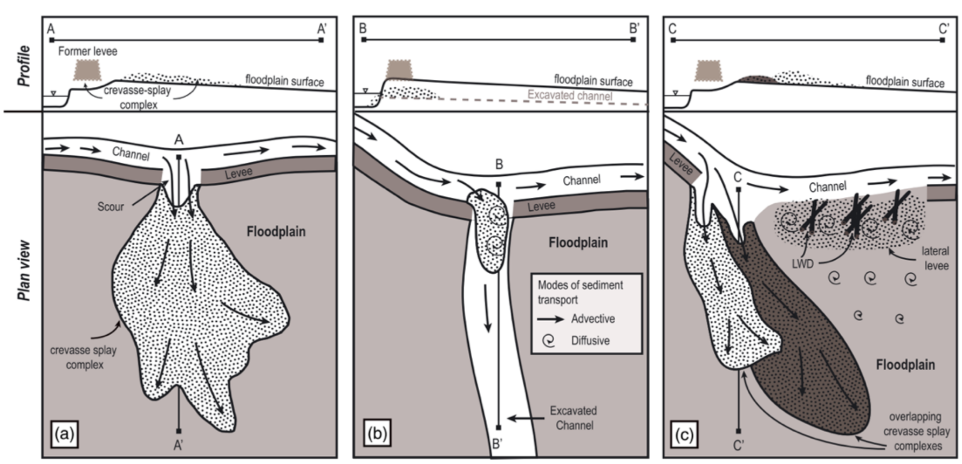

FIGURE 9 Conceptual models of floodplain topography changes to varying levee breach geometries [adapted from Florsheim and Mount (2002)]: (a) narrow breach (<75 m) opening onto a graded floodplain; (b) narrow breach (<75 m) opening into an excavated floodplain channel; (c) wide levee breach (>250 m) opening onto a graded floodplain. [Colour figure can be viewed at wileyonlinelibrary.com]

Appendix C:

Pile 1


Pile 2:

Pile 3:

Pile 4:

Pile 5:

Appendix D: